Direct Evidence for GTP and GDP-P_i Intermediates in Microtubule Assembly

Ronald Melki, Marie-France Carlier,* and Dominique Pantaloni
Laboratoire d'Enzymologie du CNRS, 91198 Gif-sur-Yvette, France
Received May 29, 1990

ABSTRACT: Identification of the kinetic intermediates in GTP hydrolysis on microtubules and characterization of their assembly properties is essential in understanding microtubule dynamics. By using an improved glass filter assay that selectively traps microtubules with a dead time of 2 s and monitoring taxol-induced rapid assembly of microtubules from [γ-^{32}P,^{3}H]GTP–tubulin 1:1 complex, direct evidence has been obtained for GTP– and GDP-P_i–microtubule transient states in the early stages of the polymerization process. A simple kinetic analysis of GTP hydrolysis on microtubules within two sequential pseudo-first-order processes led to apparent first-order rate constants of 0.065 s^{-1} for the cleavage of the γ-phosphate and 0.02 s^{-1} for the liberation of P_i, assuming a simple random model. Apparent rate constants for GTP hydrolysis and P_i release were independent of the composition of the buffer used to polymerize tubulin. The significance of these values with respect to those derived from previous studies from this and other laboratories and the possibility of a vectorial model for GTP hydrolysis are discussed.

It is well accepted that GTP hydrolysis accompanying tubulin polymerization plays a crucial role in microtubule dynamics and that uncoupling between GTP hydrolysis and microtubule assembly results in the formation of a dynamic GTP cap at the ends of microtubules, whose fluctuations are responsible for the properties of nonlinear dependence of the rate of growth on tubulin concentration, dynamic instability, and oscillatory behavior typical of a system subject to phase transitions [Hill & Carlier, 1983; Carlier et al., 1984, 1987a; Mitchison & Kirschner, 1984; Hill, 1985, 1987; Horio & Hotani, 1986; Walker et al., 1988; for review, see Carlier (1989)].

While a consensus has been reached, from independent experiments using different technologies, about the existence of a GTP cap at microtubule ends and its role in microtubule dynamics, no definite agreement exists about the size of this GTP cap at different stages of microtubule growth; in other words, the detailed mechanism of GTP hydrolysis in microtubule assembly still is a controversial and elusive issue (Carlier & Pantaloni, 1981; Hamel et al., 1984; O'Brien et al., 1987; Carlier et al., 1987b; Schilstra et al., 1987; Caplow et al., 1988a,b). The situation has been further complicated by the following recent results. By using structural analogues of P_i, the putative kinetic intermediate in which GDP-P_i is bound to microtubules, i.e., in which cleavage of GTP has occurred but P_i has not been released in solution, could be reconstituted and characterized. The finding that GDP-P_i–microtubules are very stable, i.e., lose subunits at a very slow rate, led to the conclusion that P_i release, and not cleavage of GTP, was the key step inducing a conformational change of polymerized tubulin coupled to the destabilization of the microtubule lattice (Carlier et al., 1988, 1989). In addition to the GTP cap, the potential existence of a stabilizing GDP-P_i cap at microtubule ends had to be considered, according to the following improved kinetic scheme for GTP hydrolysis on microtubules (MT):

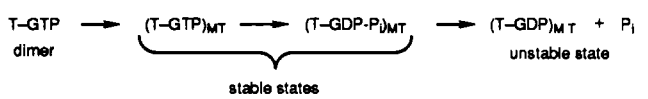

To propose a realistic analysis of microtubule dynamics in vitro and to anticipate possible modes of regulation in vivo, it is necessary to know (i) the lifetimes of the GTP and GDP-P_i intermediates on microtubules and (ii) the kinetic mechanisms of GTP cleavage and P_i release.

A kinetic experimental approach to the mechanism indicated that GTP cleavage proceeded vectorially toward the distal growing end of the microtubule (Carlier et al., 1987b). On the other hand, efforts to observe directly the GTP and GDP-P_i transient states on microtubules and derive the rate constants for cleavage of GTP and liberation of P_i have been unsuccessful (Carlier, 1988; Stewart et al., 1989), which indicated that both reactions were too fast for the potential GTP and GDP-P_i transients to be trapped efficiently by using methods that had a dead time of about 20 s. Whether a large number of tubulin subunits of the microtubule do or do not carry GTP and/or GDP-P_i transiently is an important issue when one has to decide which type of model for the cap is able to describe microtubule dynamics adequately in a large range of monomer concentrations, i.e., in a broad spectrum of rates of growth and at steady state. Indeed the possibility has been evoked (O'Brien et al., 1987; Walker et al., 1988), but also rejected (Caplow et al., 1988a,b), that in a range of concentration of GTP–tubulin the stabilizing cap of GTP subunits might consist of as few as one or two terminal GTP subunits by the elongating site that would never hydrolyze GTP. The same model had previously been proposed—and an analytical solution had been developed—for actin (Pantaloni et al., 1985; Hill, 1986), to account for the observed coincidence, at low rates of growth, between the monomer concentration dependences of the rates of F-actin filament elongation and ATP hydrolysis, at a time when the stable F-ADP-P_i–actin transient state had not been discovered.

Two conditions have to be achieved for the experimentalist to have a chance to directly observe putative long stretches of GTP– and GDP-P_i–subunits on microtubules: (1) microtubule assembly must proceed at a fast rate compared to GTP hydrolysis, and (2) microtubules must be separated from the bulk solution and trapped, for identification of the bound nucleotide, within the shortest possible time. We have tried to meet these conditions and designed a new rapid glass fiber filter assay combined with taxol-induced polymerization of double-labeled [γ-^{32}P,^{3}H]GTP–tubulin. By using this assay, direct evidence can be shown for appreciable amounts of GTP– and GDP-P_i–tubulin as transients in microtubule assembly. Because microtubule dynamics in vitro is known to be affected

0006-2960/90/0429-8921$02.50/0

by solvent composition, experiments have been carried out both in MES buffer containing 4 M glycerol and 6 mM Mg^{2+} ions (MGM buffer) and in PIPES buffer containing no glycerol and 1 mM Mg^{2+} ions (PM buffer).

Materials and Methods

Chemicals. GTP was purchased from Boehringer Mannheim, EGTA (ethylene glycol bis[β-aminoethyl ether]-*N*,*N*,*N*′,*N*′-tetraacetic acid) and PIPES (piperazine-*N*,*N*′-bis-[2-ethanesulfonic acid]) were from Sigma, MES [2-(*N*-morpholino)ethanesulfonic acid] was from Calbiochem, and colchicine was from Prolabo. Taxol purified from *Taxus baccata* (Wani et al., 1971) was a gift from D. Guénard. [^{3}H]GTP, [γ-^{32}P]GTP, [^{3}H]glucose, and $^{32}P_i$ came from Amersham. All other chemicals were Merck's analytical grade.

Tubulin. Pure tubulin was prepared from fresh pig brain by three assembly–disassembly cycles according to Shelanski et al. (1973), followed by phosphocellulose (Whatmann P11) chromatography (Weingarten et al., 1975). Tubulin was concentrated by ultrafiltration and stored at −80 °C in MG buffer (0.05 M MES, pH 6.8, 0.5 mM EGTA, 0.25 mM $MgCl_2$, and 4 M glycerol) supplemented with 100 μM GTP.

Tubulin–colchicine complex was prepared according to Sherline et al. (1974). In brief, tubulin was incubated for 30 min at 37 °C with an excess of colchicine. The unbound colchicine was removed from the solution by using activated charcoal (3 mg/mL). Tubulin (90–100 μM) in MG buffer was labeled by incubation at 0 °C for 2 h in the presence of 1 mM [γ-^{32}P,^{3}H]GTP (10 Ci of mol, [^{3}H]/20 Ci of [^{32}P]/mol). The 1:1 [γ-^{32}P,^{3}H]GTP–tubulin complex was then isolated free of unbound nucleotide by chromatography through Sephadex G-25 (PD-10, Pharmacia). The column buffer was either MG buffer or P buffer (100 mM PIPES buffer, pH 6.8, containing 1 mM EGTA and 0.1 mM $MgCl_2$) when tubulin polymerization was to be performed in the absence of glycerol. The nucleotide content of the tubulin was checked by HPLC anion-exchange chromatography with a Synchropak AX300 column (Synchrom, Inc.) and isocratic elution by 0.35 M KH_2PO_4 buffer, pH 3.5, containing 1.3 M NaCl.

The concentration of the GTP–tubulin 1:1 complex was determined spectrophotometrically by using an extinction coefficient of 1.2 mg·cm^2 at 277 nm (Detrich et al., 1979) and a molecular weight of 100 kDa (Krauhs et al., 1981).

Polymerization Measurements and Simultaneous GTPase Measurements. Tubulin polymerization was monitored turbidimetrically by using a 2-mL cuvette (optical path 1 cm) with either MGM buffer (MG buffer supplemented with 5 mM $MgCl_2$) or PM buffer (P buffer supplemented with 0.9 mM $MgCl_2$). The turbidity of the unpolymerized tubulin solution was first recorded. Then the empty cell was preheated in a water bath at 60 °C before addition of taxol (from a 1 mM solution in DMSO) followed by (time zero) 1.5 mL of ice-cold [γ-^{32}P,^{3}H]GTP–tubulin (30 μM) in MGM or PM buffer. Mixing was ensured by vigorous pipetting. The final concentration of taxol was 30 μM in the polymerization assay in MGM buffer and 55 μM in the polymerization assay in PM buffer (see Results for the optimization of the assay). In the presence of taxol, assembly started before the temperature reached 37 °C (Thompson et al., 1981). At 8 s, the temperature of the solution had reached 30 °C and the cuvette was immediately transferred to the cell compartment of a Cary 219 spectrophotometer thermostated at 37 °C. Turbidity was recorded while 40-μL aliquots of the solution were withdrawn from the cuvette at time intervals and immediately transferred into 1.5 mL of ice-cold 10 mM ammonium molybdate in 1 N HCl for determination of acid-labile P_i, as described previously (Carlier & Pantaloni, 1981; Carlier et al., 1987a). Emphasis has been given (Carlier, 1989) on the adequacy of this classical procedure, as opposed to the poor results obtained (O'Brien et al., 1987) when 4 N H_2SO_4 was used instead of 1 N HCl. At the time of the first reading (10 s), turbidity had reached 80% of the plateau value. The amount of tubulin polymerized at the plateau was determined by sedimentation in an Airfuge (Beckman).

Glass Fiber Filter Assay. A filter assay was designed to follow polymerization under kinetic conditions as close as possible to those of the turbidity assay. Taxol (16.5 or 30.3 μL from a 10 mM solution in DMSO, according to whether polymerization was carried out in MGM or PM buffer) was placed in the bottom of a 6-mL glass tube preheated at 60 °C for 3 min. At time zero of the experiment, 5.5 mL of ice-cold [γ-^{32}P,^{3}H]GTP–tubulin (30 μM in MGM or PM buffer) was poured in the tube at 60 °C. Repeated pipetting with the 5-mL pipet tip of a P-5000 Gilson pipet ensured mixing and a homogeneous rise in temperature, which reached 30 °C within 11 s. At this time the tube was rapidly transferred to a nearby water bath thermostated at 37 °C. At different time intervals between 13 and 200 s, aliquots of 500 μL were pipetted off the tube by using a heated pipet tip and placed in a 5-mL syringe equipped with a 10-mm Swinnex holder (Millipore) containing two GFF glass fiber filters (Whatman). Filtration was performed in 2 s. Each time noted was the filtration time. The combined syringes and filters apparatus were prepared in advance and maintained in a 37 °C chamber placed close to the tube in which polymerization was carried out, for fast manipulation.[1] The filters had been first treated with 1 mL of BSA (2 mg/mL in MGM or PM buffer) to reduce the adsorption of tubulin dimer. At the end of the experiment, the filters were removed from the Swinnex holder and put in scintillation vials. The filters were then incubated with 0.5 mL of 0.1 N NaOH for 30 min prior to the addition of 10 mL of Aquasol. Radioactivity (^{3}H and ^{32}P) was measured in a Packard CA 2000 scintillation spectrometer. The time course of assembly was derived from the increase in ^{3}H radioactivity present in the filter (i.e., total bound nucleotide, GTP + GDP-P_i + GDP). The increase in the amount of ^{32}P present in the filter corresponded to GTP + GDP-P_i bound to microtubules.

Because assembly proceeded so fast in this assay, the determination of ^{3}H and ^{32}P radioactivity at time zero of assembly required that the same sample be maintained unpolymerized under the same physical conditions as in the assembly assay. For this purpose, tubulin in the presence of Mg^{2+} and 9 μM tubulin–cholchicine complex was brought to 37 °C in the same way as in the assay, except in the absence of taxol. It was checked by turbidimetry that under these conditions GTP–tubulin did not assemble into microtubules for minutes.

Alternatively, the zero time point was obtained by filtering the labeled tubulin solution at 37 °C in MG or P buffer containing no taxol. The amount of Mg^{2+} ions in MG and P buffers was too low to allow polymerization of tubulin.

Electron Microscopy. Microtubule length redistribution during tubulin polymerization in the presence of taxol was

[1] Three workers were required for maximum efficiency and speed in this experiment: one person carried out the two incubations and pipetting of aliquots at time intervals, another one operated the rapid filtration of each sample, and the third one watched the chronometer and noted the filtration times.

followed by electron microscopy of negatively stained samples by using a Philips EM 410 instrument. Carbon-coated grids (200 mesh) were deposited on a drop of sample at different times of the reaction, washed rapidly 5 s later, and immediately deposited on a drop of 1% uranyl acetate.

RESULTS

Design and Optimization of the Filter Assay: Adsorption of the Different Components of the System (Tubulin, Microtubules, and Inorganic Phosphate) on GFF Filters. In a previous glass filter assay (Carlier, 1988) developed after Wilson et al. (1982), 50-μL aliquots of the microtubule solution were removed at different times of assembly and extensively diluted (80-fold) in a quench solution containing 8 M glycerol and glutaraldehyde before filtration. The dead time involved in this method was 20 s. In the new assay described under Materials and Methods, dilution in a quenching and fixing solution is avoided, which reduces the dead time to 2 s. In addition, in this new assay the absence of unbound nucleotide has two advantages: first, it avoids the complication of the adsorption of free labeled GTP on the glass filter, and second, the GTP–tubulin 1:1 complex can undergo only one cycle of assembly (single-turnover experiment); therefore, the analysis of GTP hydrolysis during microtubule assembly is simpler in the absence of the interfering steady-state GTPase reaction, which was a complication in previous work (Carlier & Pantaloni, 1981). The presence of taxol in the assay also has two advantages: first, it guarantees that practically all the tubulin assembles in microtubules at a fast rate with a very large number of short microtubules, which are choice conditions for the potential observation of transient states of GTP hydrolysis on polymerized tubulin, and second, taxol stabilizes the GDP–microtubules resulting from a single round of assembly in the absence of free GTP, while they would spontaneously disassemble under these conditions in the absence of taxol (Carlier & Pantaloni, 1978). In summary, the rationale of this assay was to be as close as possible to the experimental conditions used to examine the sequence of intermediate complexes formed in an enzyme + substrate single-turnover reaction. However, in this new assay the interference of the radioactive label nonspecifically adsorbed on glass and trapped in the interstitial volume of the glass fiber filter becomes more important. Also, the absence of fixation makes microtubules more labile and may reduce their retention on the filter. The importance of these problems and the possible limitations of the assay were first assessed in the following experiments.

The different adsorption coefficients of tubulin and microtubules were measured by filtering 500 μL of the 1:1 [^{3}H]GTP–tubulin complex at different concentrations in MGM buffer prepared at 37 °C, either in the microtubule state upon addition of an equimolar amount of taxol or in the dimeric state (either in the absence of Mg^{2+} or upon addition of a 30% amount of tubulin–colchicine). Filtration was done 1 min after the temperature had been raised to 37 °C. The amount of total and adsorbed material was determined by measuring ^{3}H radioactivity. In the presence of taxol, 90% of the tubulin was assembled in microtubules as measured by sedimentation. The results of this experiment are displayed in Figure 1 and show that, in a range of tubulin concentrations from 0 to 40 μM, 23% of the dimeric tubulin in the presence of tubulin–colchicine complex and 61% of the microtubules are retained on the filters. When dimeric tubulin was filtered in MG buffer that contained only 0.5 mM $MgCl_2$, 8% of the tubulin adsorbed to the filter. This value is lower than the 23% obtained above in the presence of 6 mM Mg^{2+} and colchicine; however, in the absence of millimolar amounts of

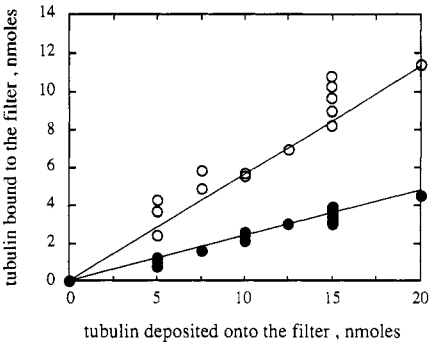

FIGURE 1: Adsorption of dimeric tubulin and microtubules on glass fiber filters. Solution of [^{3}H]GTP–tubulin (1:1 complex) at different concentrations (0–40 μM) in MGM buffer were prepared at 37 °C in the presence of either 30% tubulin–colchicine (dimer tubulin, ●) or 1 equiv of taxol (microtubules, ○). After a 1-min incubation at 37 °C, aliquots of 500 μL (i.e., containing 0–20 nmol of [^{3}H]GXP-labeled tubulin) were filtered as described under Materials and Methods. The amount (in nmol) of tubulin trapped on the filter is plotted versus the amount of filtered tubulin. Data coming from independent experiments are superimposed.

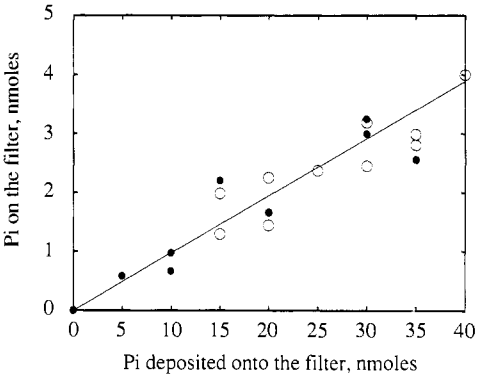

FIGURE 2: Adsorption of P_i on glass fiber filters, in the presence of tubulin or microtubules. Different amounts of $^{32}P_i$ were added to solutions of GTP–tubulin (1:1 complex, 30 μM) either polymerized for 2 min in MGM buffer, in the presence of an equimolar amount of taxol, or maintained unpolymerized by addition of 9 μM tubulin–colchicine. Aliquots (500 μL) of each sample were filtered at 37 °C. In the calculation of $^{32}P_i$ specific radioactivity, the presence of endogenous 30 μM P_i coming from hydrolysis of GTP was taken into account in the microtubule sample. On the other hand, it was checked that none of the GTP was hydrolyzed in the dimer tubulin sample following a 1-min incubation with tubulin–colchicine. The amount of P_i retained on the filter in the samples containing dimeric tubulin (●) or microtubules (○) is plotted versus the total amount of P_i present in the filtered sample.

Mg^{2+}, the conformation of dimeric tubulin may be different and cause a lower adsorption to the filter. Therefore, the Mg–colchicine filtration assay was thought to provide a better, although more pessimistic, estimate of the time zero of the experiment.

A second piece of information needed in the analysis of the data is the adsorption of inorganic phosphate on the filters in the presence of either dimeric tubulin or microtubules. This was measured by filtering 500 μL of a 30 μM GTP–tubulin solution (either dimeric with 9 μM tubulin–colchicine present or polymerized for 2 min in the presence of 30 μM taxol) containing different amounts of $^{32}P_i$. The data (Figure 2) show that in the range 0–80 μM P_i, 10% of the filtered P_i remains bound to the filter in the presence of either tubulin or microtubules at 30 μM. A similar experiment (data not shown) was done with [^{3}H]glucose in the place of inorganic phosphate. In the same range of concentration, 9.4–10.6% of the [^{3}H]-glucose was found bound to filters in the presence of tubulin and microtubules, respectively. These numbers indicate that

the interstitial volume of the filters represents 10% ± 1% of the filtered volume, i.e., 50 ± 3 μL, and that P_i in the range 0–80 μM does not appreciably adsorb to the glass filter nor to microtubules, in agreement with its measured low affinity (Carlier et al., 1988; Caplow et al., 1989).

Together the results of Figures 1 and 2 demonstrate that the filtration assay as defined should be feasible to follow polymerization of the 1:1 [γ-^{32}P,^{3}H]GTP–tubulin complex in the presence of taxol. The change in [^{3}H] bound to the filter during polymerization can be used to monitor the polymerization process, according to the equation:

$$[^3H]_{filter} = f_{Tub}[T\text{–}[^3H]GTP] + f_{MT}[T_{pol}\text{–}[^3H]GXP] \quad (1)$$

where [T–[^{3}H]GTP] and [T_{pol}–[^{3}H]GXP] represent the amounts of dimeric and polymerized tubulin present in the filtered sample and f_{Tub} and f_{MT} represent the adsorption coefficients of dimeric tubulin and microtubules on the glass filter.

Since the total amount of tubulin present in the sample is Q_0 = [T–[^{3}H]GTP] + [T_{pol}–[^{3}H]GXP], eq 1 can be written

$$[^3H]_{filter} = f_{Tub}Q_0 + (f_{MT} - f_{Tub})[T_{pol}\text{–}[^3H]GXP] \quad (2)$$

The amount of ^{3}H radioactivity on the filter therefore increases with microtubule formation with a proportion coefficient equal to $f_{MT} - f_{Tub}$:

$$(MT) = [T_{pol}\text{–}GXP] = ([^3H]_{filter} - f_{Tub}Q_0)/(f_{MT} - f_{Tub}) \quad (3)$$

Figures 1 and 2 show that f_{MT} = 0.61 and f_{Tub} = 0.23.

A similar equation can be derived for [^{32}P] bound to the filter:

$$[^{32}P]_{filter} = f_{Tub}[T\text{–}[^{32}P]GTP] + f_{MT}([T_{pol}\text{–}[^{32}P]GTP] + [T_{pol}\text{–GDP-}^{32}P_i]) + f_{P_i}[^{32}P_i] \quad (4)$$

Since [P_i] = [T_{pol}–GDP], eq 4 can be rearranged:

$$[^{32}P]_{filter} = f_{Tub}Q_0 + (f_{MT} - f_{Tub})[T_{pol}\text{–GXP}] - (f_{MT} - f_{Pi})[T_{pol}\text{–GDP}] \quad (5)$$

The first two terms in the above equation are equal to the amount of ^{3}H bound to the filter (eq 2). Hence

$$T_{pol}\text{–GDP} = ([^3H]_{filter} - [^{32}P]_{filter})/(f_{MT} - f_{Pi}) \quad (6)$$

Comparison of the time courses for whole microtubule formation, derived from $[^3H]_{filter}$, and GDP–microtubule formation, derived from $[^{32}P]_{filter}$, leads to the time course of GTP + GDP-P_i transient microtubule species. Further comparison with the kinetics of cleavage of the γ-phosphate leads to the deconvolution of all intermediates in microtubule assembly.

Optimization of the Concentration of Taxol Used in the Assay. The presence of taxol in this assay ensures the rapid nucleation of a large number of microtubules and their stabilization following hydrolysis of GTP. The possible pitfall of the introduction of taxol is the burst formation of mixed short closed microtubules and short flat microtubular sheets made of 6–10 adjacent protofilaments, which show a tendency to twist. It is known (Berne, 1974) that such objects of length shorter than 1 μm scatter light less than long microtubules. In addition, taxol has been reported to cause slow bundling of microtubules (Wilson et al., 1985), which is known to cause the enhancement of light scattering (Huitorel et al., 1985). The effect of increasing taxol concentration on the turbidimetric recording of the polymerization of GTP–tubulin 1:1

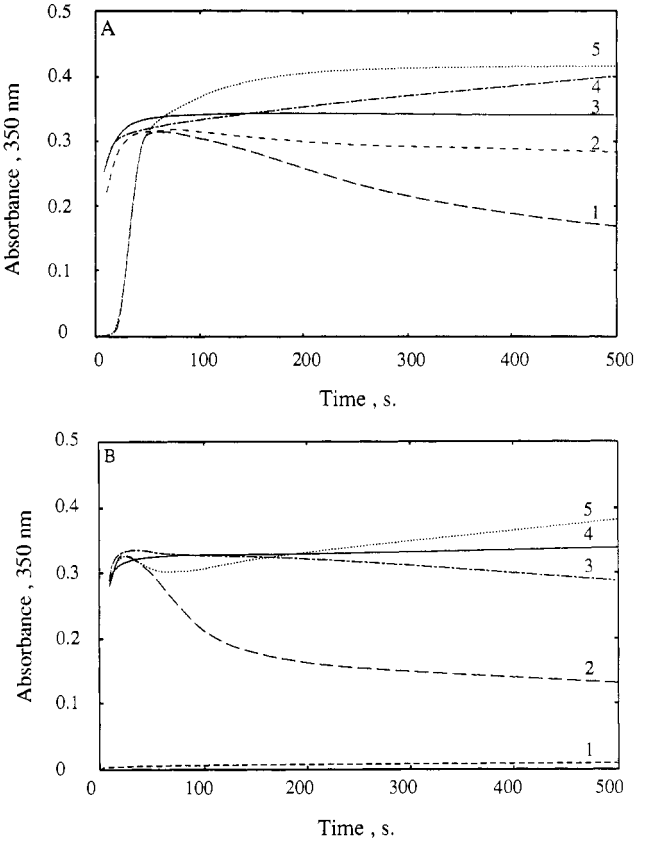

FIGURE 3: Stabilization by taxol of microtubules assembled from GTP–tubulin in the absence of free GTP, in MEM and PM buffers. GTP–tubulin 1:1 complex was polymerized at 30 μM in MEM buffer (Panel A) and PM buffer (Panel B) in the absence of free GTP and the presence of taxol at the following concentrations (in μM): panel A, curve 1, 0; curve 2, 25; curve 3, 30; curve 4, 35; curve 5, 0, 100 μM free GTP; panel B, curve 1, 0; curve 2, 30; curve 3, 45; curve 4, 55; curve 5, 60. Turbidity at 350 nm was recorded (light path 0.5 cm).

complex (30 μM) in MGM and PM buffers is shown in Figure 3, panels A and B, respectively. In glycerol-containing buffer (MGM), microtubules assembled in the absence of taxol and then depolymerized spotaneously once GTP was consumed, as previously observed (Carlier & Pantaloni, 1978). The presence of 1 molar equiv of taxol was enough to polymerize tubulin within 20 s and stabilize GDP–microtubules. Increasing taxol concentration above 1 equiv/tubulin resulted in a slow increase in turbidity following the rapid burst of assembly. The extent of turbidity change in the presence of taxol was 77% of the increase measured under standard conditions (absence of taxol, presence of free GTP), in agreement with our previous observations (Carlier & Pantaloni, 1983). In PM buffer (no glycerol present, Figure 3B), no spontaneous nucleation was observed in the absence of taxol. One molar equivalent of taxol per tubulin was not sufficient, in this buffer, to stabilize GDP–microtubules in the absence of GTP. The optimum concentration of taxol was 55 μM.

Identification of Short Microtubules and Microtubular Sheets Formed upon Taxol-Induced Rapid Assembly of Microtubules. In order to check that the reactions of GTP hydrolysis and P_i release that have been measured take place on tubulin in a microtubular lattice and not on nonmicrotubular aspecific aggregates, electron microscopy of the polymerizing species was carried out at different stages of the assembly process. Figure 4 shows that in the early stages of assembly (t = 10–20 s), short (8–10 protofilaments wide) microtubular flat sheets, narrow sheets (6 protofilaments wide) forming twisted ribbons, and short closed microtubules were

the only polymerized forms of tubulin in both MGM and PM buffers. The identical microtubular nature of tubulin–tubulin interactions in these early polymers has been documented (Voter & Erickson, 1984). Note that all these polymers are of small size and different from the large sheets (15–25 protofilaments wide, over 1 μm long) reported to cause a transient overshoot in the turbidity recording of the polymerization of tubulin from sea urchin egg (Detrich et al., 1985). In the present case, the short polymers observed actually scatter light less than long microtubules, as illustrated in Figure 3. At later stages of assembly, longer microtubules were observed. Therefore, in the presence of taxol following GTP hydrolysis, length redistribution and/or end-to-end association of short GDP–microtubules occurs (Carlier & Pantaloni, 1983; Williams & Rone, 1989). A histogram of length distribution of 305 microtubules and flat sheets (Figure 4E) shows an average length of 0.43 μm. However, because it is difficult to estimate the size of twisted ribbons, these polymers were not counted, which introduces a bias in the analysis, since twisted ribbons represent ~25% (in number) of the polymerized species observed on the grid.

Cleavage of the γ-Phosphate of GTP during Taxol-Induced Rapid Assembly of Microtubules. The formation of acid-labile $^{32}P_i$ resulting from the chemical cleavage of [γ-^{32}P]GTP was measured during the rapid polymerization of 30 μM GTP–tubulin 1:1 complex in the presence of 30 μM taxol. The polymerization reaction was monitored turbidimetrically while aliquots were taken off the cuvette for the GTPase assay. Figure 5 shows that the assembly reaction proceeded faster than GTP hydrolysis. The difference between the two time courses represents the transient GTP bound to microtubules. Assembly was 100% complete in 20 s, and at the same time 50% of the microtubule consisted of GTP–subunits.

A slow 10% decrease in turbidity, due to the instability of GDP–microtubules, occurred between 30 and 120 s. This decrease is very slow here due to the presence of stabilizing taxol. As a result, the turbidity curve and the GTP cleavage curve cross each other at 60 s, because turbidity reflects the combination of association and dissociation events, while GTP hydrolysis is simply cumulative. For this reason, the amount of GTP transiently bound to microtubules can be determined with accuracy only during the net assembly phase, i.e., between 0 and 60 s. After 60 s of assembly, GTP–microtubules represent a very low proportion of microtubules (e.g., $\ll$5%).

Evidence for GTP and GDP-P_i Transiently Bound to Microtubules in the Early Stages of Assembly. (A) Polymerization in Glycerol-Containing Buffer (MGM). Rapid assembly of the [γ-^{32}P,^{3}H]GTP–tubulin 1:1 complex (30 μM) in the presence of an equimolar amount of taxol was monitored by using the filter assay as described under Materials and Methods. Raw data showing the evolution with time of ^{3}H and ^{32}P bound to the filter in two typical experiments in MGM buffer are displayed in Figure 6, panels A and C. The main observations are the following: (1) The ^{3}H radioactivity on the filter shows a continuous increase and reaches a plateau at 20–30 s (with a subsequent 10% decrease within the following 120 s). This observation is consistent with turbidity data. (2) The ^{32}P radioactivity shows an increase simultaneous with the increase in ^{3}H, followed by a decrease. The maximum in ^{32}P bound to the filter occurred at 20–30 s, and the half-time for the decrease was at 50 s. The increase in ^{3}H bound to the filter represents microtubule formation, i.e., the sum of the amounts of polymerized GTP–, GDP-P_i–, and GDP–tubulin; the increase then decrease in ^{32}P bound to the filter was repeatedly observed in a large number of experiments and is a straightforward indication for the transient formation of polymerized GTP– and GDP-P_i–tubulin, followed by P_i release. The time courses of total microtubule, GTP + GDP-P_i intermediates, and GDP–microtubule formation can be derived from the raw data according to eqs 2 and 6 and are shown in Figure 6, panels B and D. A combination of data from Figures 5 and 6 leads to the complete deconvolution of the sequence of microtubule intermediates during polymerization. The time courses of total polymer (given by turbidity as well as by ^{3}H bound to the filter) and of GTP–, GDP-P_i–, and GDP–microtubules are superimposed in Figure 7.

The data show that the simple existence of a GTP–microtubule transient cannot account for the lifetime of ^{32}P, coming from [γ-^{32}P]GTP, on microtubules and that another intermediate, GDP-Pi–microtubules, exists, with a longer lifetime than GTP–microtubules.

In Figure 7, the data have been corrected for the slow depolymerization that occurs after 50 s, to simplify the mathematical analysis. That is, the amount of GDP– and GDP-P_i–microtubules at each time (t > 50 s) was divided by the whole amount of microtubules measured at the same time.

The maximum in GTP bound to microtubules is at 15 s, at which time GTP–subunits represent 60% of the microtubule, while the maximum in GDP-P_i is reached at 30–40 s, at which time GDP-P_i–subunits represent 25% of the microtubule.

(B) Polymerization in Low Mg^{2+}, No Glycerol Buffer (PM Buffer). The filter assay was carried out in PM buffer, which is the buffer used for videomicroscopy observations of dynamic instability of individual microtubules (Walker et al., 1988) and in which recent electron microscopy observations (Karecla et al., 1989) indicate that more closed microtubules and less flat sheets are formed.

The adsorption coefficients of tubulin dimers (in the absence of Mg^{2+}), of taxol microtubules and of P_i on GFF filters were first measured in PM buffer. The following values were found: $f_{Tub} = 0.065$, $f_{MT-GDP} = 0.125$, and $f_{Pi} = 0.05$. These numbers show that in PM buffer microtubules adsorb very poorly to the glass filter. Despite this difficulty, the filter assay was carried out in order to determine whether the rates of GTP hydrolysis and P_i release would be appreciably sensitive to the nature of the buffer. Data from a typical experiment are displayed in Figure 8. Panel A shows the raw data of the filter assay, and panel B shows the combination of treated filter data with turbidity and simultaneous GTP hydrolysis measurements. It appears that in this buffer too a satisfactory agreement was obtained between the increase in ^{3}H on the filter and the increase in turbidity, showing that tubulin polymerization was completed within 50 s. However, the amount of ^{3}H radioactivity on the filter decreased more appreciably with time than in MGM buffer, in parallel with P_i release, indicating that, consistent with the results in Figure 3B, in PM buffer GDP–microtubules were unstable upon filtration, even in the presence of 55 μM taxol.

(C) Polymerization of GTP–Tubulin 1:1 Complex in the Absence of Taxol. A final control was made to check that the transient GDP-P_i polymer species observed was not artifactually either due to the presence of taxol or bound to a nonmicrotubular irrelevant structure undetectable by electron microscopy. Double-labeled GTP–tubulin 1:1 complex (30 μM) was therefore polymerized in the absence of taxol in MGM buffer. Only 2–3-μm-long microtubules were observed at the turbidity maximum (t = 60 s). Figure 9 shows that in this case too a measurable transient amount of ^{32}P-labeled microtubules can be observed. This amount is lower than when taxol is present because of the slower polymerization. How-

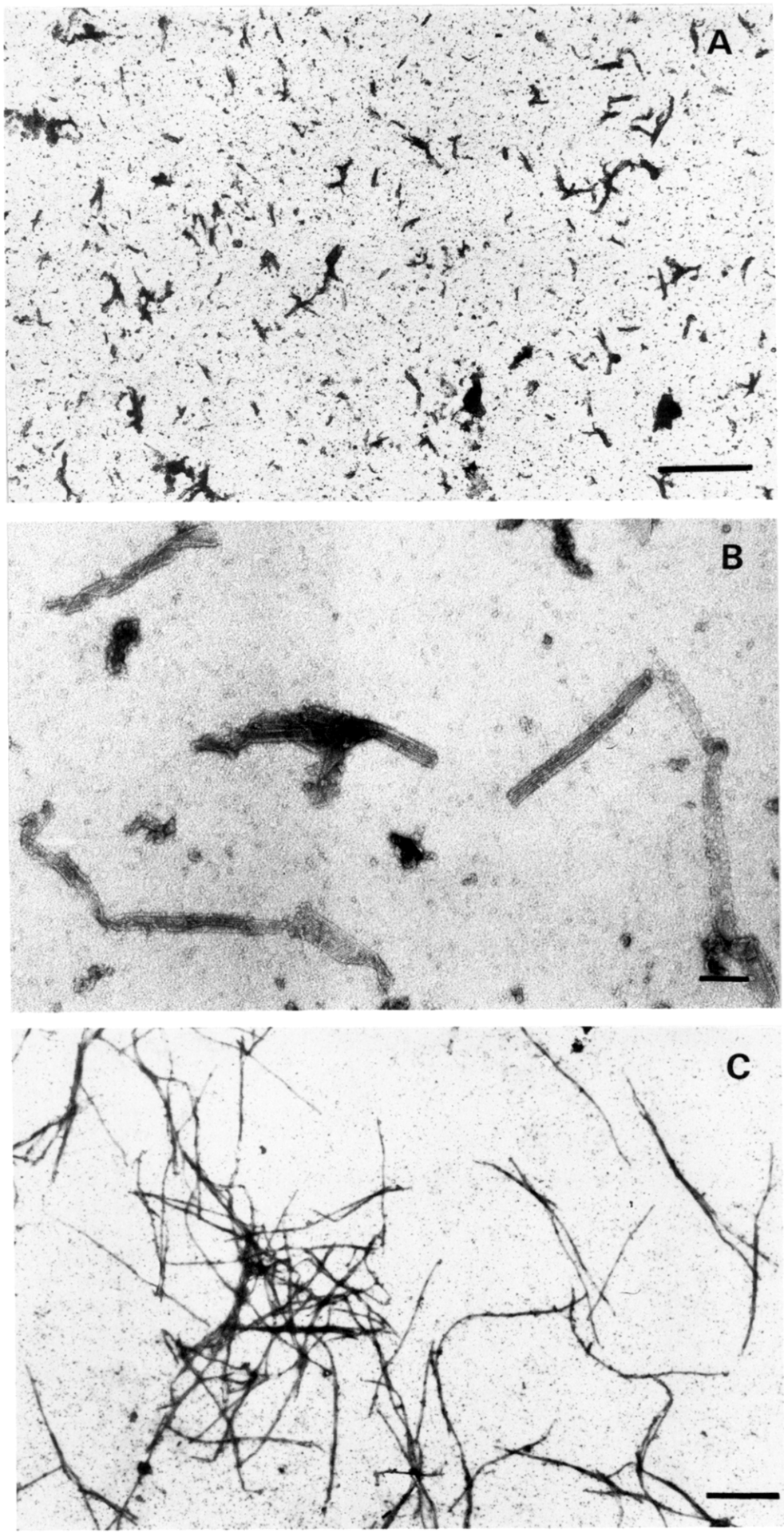
A
B
C

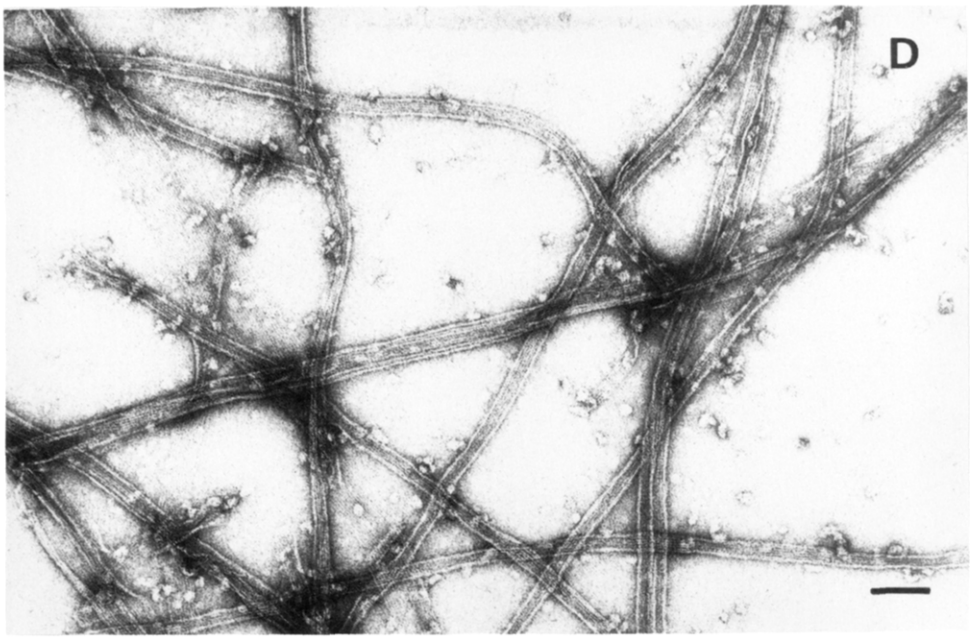

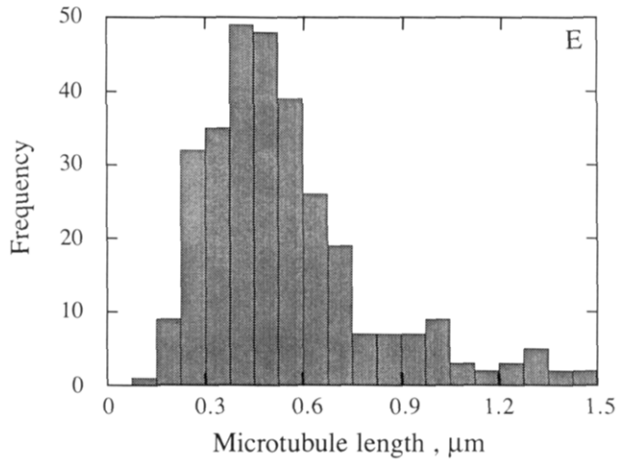

FIGURE 4: Electron microscope identification of microtubules in the early and late stages of the rapid assembly of GTP–tubulin. Low magnification (panels A and C; bar = 1 μm) and high magnification (panels B and D; bar = 0.1 μm) of the assembled species at time 10 s (panels A and B) and 150 s (panels C and D) of the rapid polymerization of GTP–tubulin in MGM buffer. Panel E: Histogram of length distribution of short microtubules and flat sheets formed at t = 20 s of taxol-induced polymerization of GTP–tubulin in MGM buffer. A total of 305 polymers were counted on photographs taken with a 17820-fold magnification. Twisted ribbons were not counted.

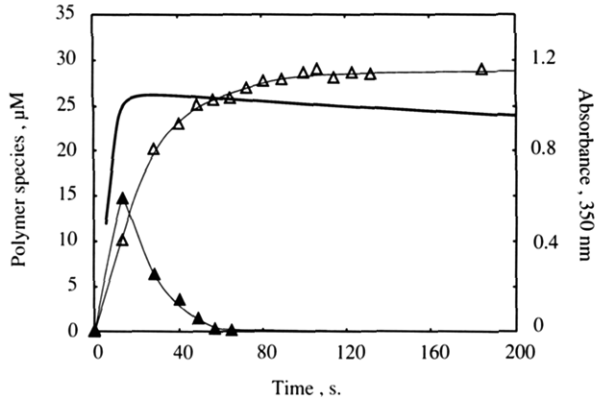

FIGURE 5: Cleavage of the γ-phosphate of GTP upon rapid assembly of GTP–tubulin (1:1 complex). A solution of [γ-^{32}P]GTP–tubulin (1:1 complex, 30 μM) was polymerized in the presence of 30 μM taxol in the preheated cuvette of the spectrophotometer as described under Materials and Methods. Aliquots were rapidly removed from the cuvette for determination of acid-labile $^{32}P_i$ (△). The difference between the polymerization curve and the GTP hydrolysis curve represents GTP bound to microtubules (▲). Solid line: turbidity recording. Polymer species refers to total microtubules (solid line), (GDPhP_i + GDP)–polymer (△), and GTP–polymer (▲).

Scheme I

ever, the ratio $^{32}P/^{3}H$ on the filter clearly decreases during polymerization. This piece of data gives confidence that the results obtained in the presence of taxol pertain to microtubules and not to aspecific aggregates.

Simple Kinetic Model for GTP Hydrolysis and P_i Release on Microtubules. In a first approximation, an attempt has been made to fit a simple model to the data, according to Scheme I. Within this scheme, k_1, k_2, and k_3 represent the pseudo-first-order rate of polymerization, the first-order rate of GTP hydrolysis, and the first-order rate of P_i liberation, respectively. It is implicitly assumed that GTP is hydrolyzed and P_i released at the same rates on all GTP subunits of the microtubule.

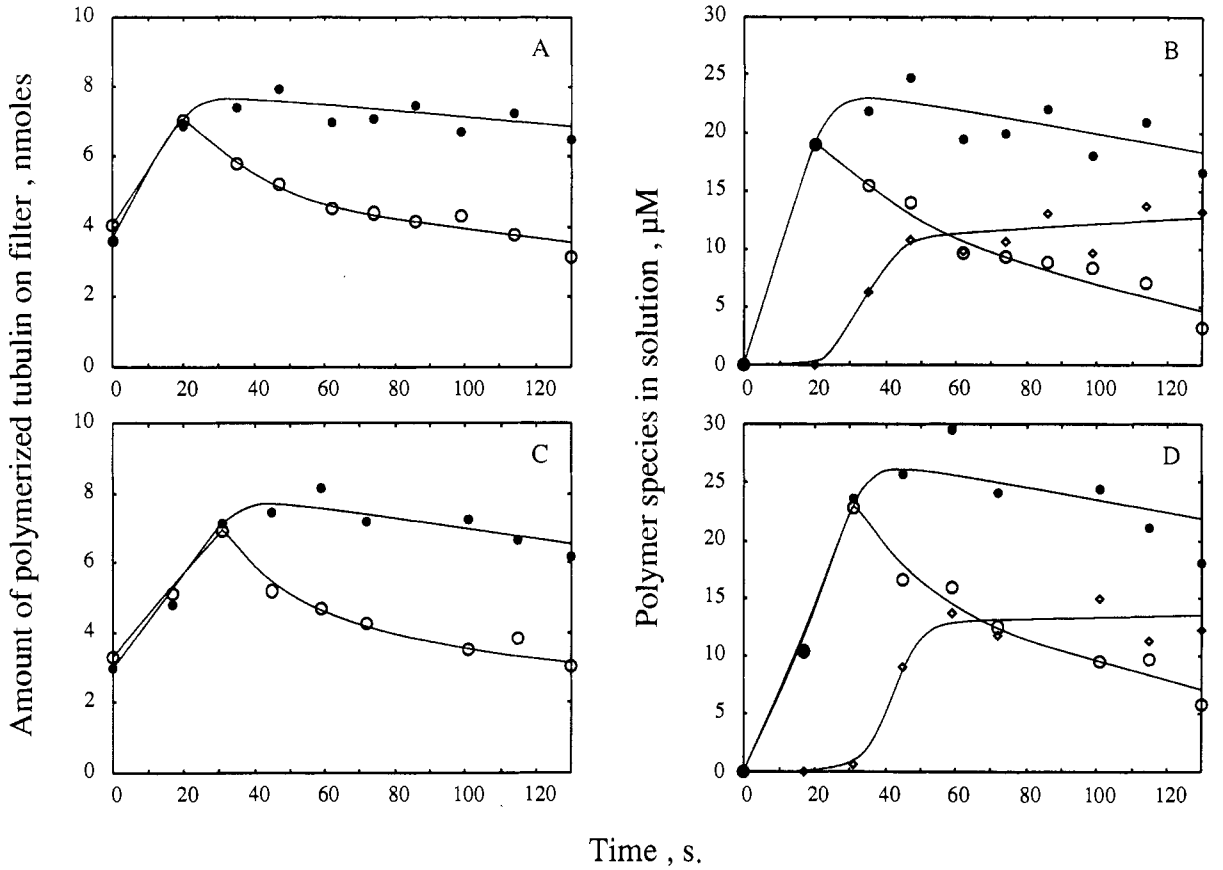

FIGURE 6: Glass filter assay for polymerization of [γ-^{32}P,^{3}H]GTP–tubulin (1:1 complex) in MGM buffer. Two identical typical experiments in which [γ-^{32}P,^{3}H]GTP–tubulin 1:1 complex (30 μM) was rapidly polymerized with 30 μM taxol as described under Materials and Methods. Left panels (A and C): raw data. The amounts of ^{3}H-labeled nucleotide–tubulin (●) and of ^{32}P-labeled nucleotide–tubulin (○) bound to the filter are plotted versus time. Right panels (B and D): analysis of the corresponding raw data according to eqs 3 and 6, showing the time courses of total (GTP + GDP-P_i + GDP)–microtubule assembly (●) derived from ^{3}H measurements and of (GTP + GDP-P_i)–microtubule (○) and GDP–microtubule (◇) formation derived from ^{32}P measurements.

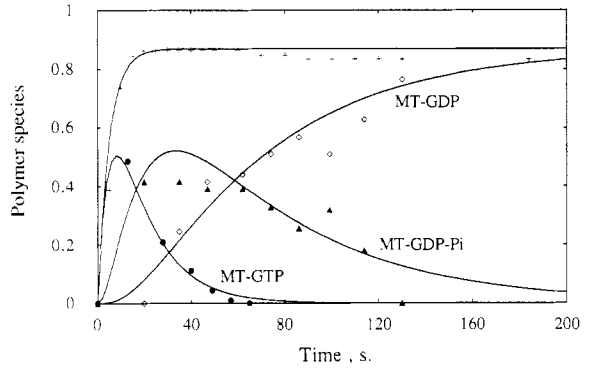

FIGURE 7: Kinetic analysis of the elementary steps in GTP hydrolysis on microtubules. Data from Figures 5 and 6 have been combined in order to show evidence for whole microtubule assembly (turbidity data, crosses): GTP–microtubules (●), GDP-P_i–microtubules (▲), and GDP–microtubules (◇). Data at times >40 s have been corrected to compensate for the slow depolymerization following GTP hydrolysis (see text). Solid lines represent theoretical curves obtained according to eqs 7–9, with the following values for the rate constants: $k_1 = 0.2$ s^{-1}, $k_2 = 0.065$ s^{-1}, and $k_3 = 0.02$ s^{-1}.

Scheme I can be described by the following system of differential equations:

$$\begin{aligned} dT/dt &= T_0 k_1 e^{-k_1 t} - k_2 T \\ dP/dt &= k_2 T - k_3 P \\ dD/dt &= k_3 P \\ T + P + D &= T_0 (1 - e^{-k_1 t}) \end{aligned} \quad (7)$$

where T, P, D, and T_0 represent the concentrations of (T–GTP)$_{MT}$, (T–GDP-P_i)$_{MT}$, (T–GDP)$_{MT}$, and total final polymer,

Table I: Rate Constants for Tubulin Polymerization and GTP Hydrolysis[a]

buffer	rate constant (s^{-1})		
	k_1	k_2	k_3
PM	0.05 ± 0.02	0.065 ± 0.007	0.02 ± 0.002
MGM	0.2 ± 0.05	0.065 ± 0.007	0.02 ± 0.002

[a] Pseudo-first-order rate of polymerization (k_1), first-order rate of GTP hydrolysis (k_2), and first-order rate of P_i liberation (k_3) values were used to fit theoretical curves to the experimental data obtained in PM and MGM buffer, assuming a random GTP hydrolysis and P_i release mechanism.

respectively. Solving the above system leads to the following equations for the evolution with time of each microtubule transient species:

$$T = T_0 \frac{k_1}{k_1 - k_2}(e^{-k_2 t} - e^{-k_1 t}) \quad (8)$$

$$P = T_0 \frac{k_1 k_2}{k_1 - k_2}\left(\frac{e^{-k_1 t} - e^{-k_3 t}}{k_1 - k_3} - \frac{e^{-k_2 t} - e^{-k_3 t}}{k_2 - k_3}\right) \quad (9)$$

Values of k_1, k_2, and k_3 were sought that would give the best adjustment of the theoretical curves 3 and 4 to the experimental data. Interestingly, only k_1 is needed to fit the polymerization curve and only k_1 and k_2 to fit the evolution of T. Therefore, very little uncertainty is possible in each value of the three rate constants. Figure 7 shows that in MGM buffer a reasonable fit can be obtained by using $k_1 = 0.2 \pm 0.05$ s^{-1}, $k_2 = 0.065 \pm 0.007$ s^{-1}, and $k_3 = 0.02 \pm 0.002$ s^{-1}, where $k_1 = k_+$[microtubules] (k_+ is the second-order association rate constant) and k_2 and k_3 represent rate constants

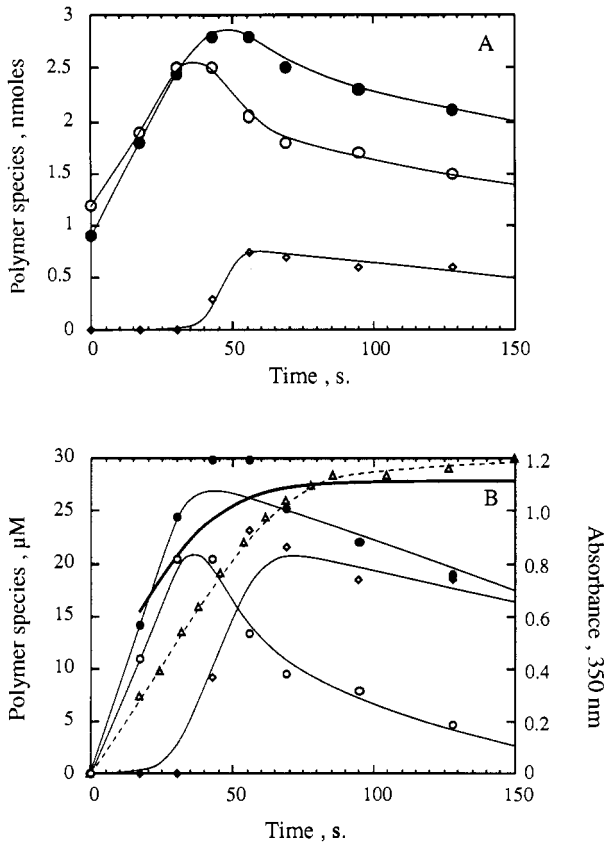

FIGURE 8: Glass filter assay for polymerization of GTP–tubulin 1:1 complex in glycerol-free buffer. [γ-^{32}P,^{3}H]GTP–tubulin 1:1 complex (30 μM) was rapidly polymerized by addition of 55 μM taxol in PM buffer. Panel A: Raw data. The evolution with time of ^{3}H-labeled nucleotide–tubulin (●) and of ^{32}P-labeled nucleotide–tubulin (○) bound to the filter are plotted. The difference between ^{3}H and ^{32}P radioactivity trapped on the filter represent the evolution with time of GDP–microtubules (◇). Panel B: Analysis of the raw data according to eqs 3 and 6, showing the time course of total microtubule assembly (●) derived from ^{3}H measurement and of GTP and GDP-P_i (○) and GDP (◇) microtubules derived from ^{32}P measurement. The turbidity recording (solid thick line) and time course of GTP cleavage (△) coming from a parallel experiment are also shown.

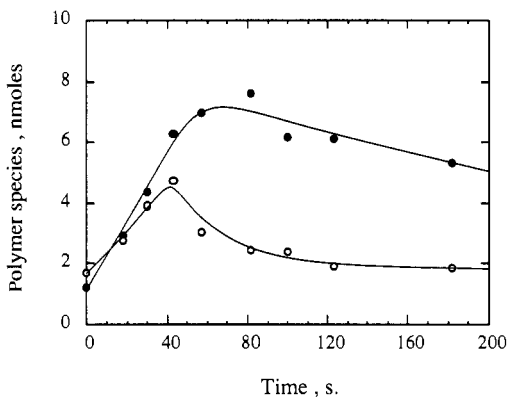

FIGURE 9: GTP and GDP-P_i transient evolution during GTP–tubulin assembly in the absence of taxol. [γ-^{32}P,^{3}H]GTP–tubulin 1:1 complex (30 μM) was polymerized in MEM buffer as described under Materials and Methods but in the absence of taxol. The evolution with time of the amounts of ^{3}H-labeled nucleotide–tubulin (●) and of ^{32}P-labeled nucleotide–tubulin (○) bound to the filter are shown. Note that although microtubule assembly is slower than in the presence of taxol, a transient increase of ^{32}P bound to the filter is observed, and the ratio [polymer-bound ^{32}P]/[polymer-bound ^{3}H] decreases with time.

for GTP hydrolysis and P_i release, assuming a random mechanism. The best fit to the data obtained in PM buffer (Figure 8) was found by using $k_1 = 0.05 \pm 0.02$ s^{-1}, $k_2 = 0.065 \pm 0.007$ s^{-1}, and $k_3 = 0.02 \pm 0.002$ s^{-1}. This fit is illustrated in Figure 9. The values of all rate constants for polymerization and nucleotide hydrolysis are summarized in Table I. It appears that the rates of GTP cleavage and P_i release are insensitive to the content of the buffer in glycerol and Mg^{2+} ions.

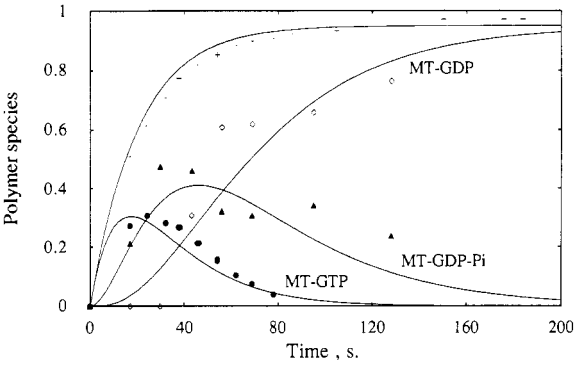

FIGURE 10: Kinetic analysis of the elementary steps in GTP hydrolysis on microtubule in glycerol-free buffer (PM buffer). Data from Figure 8B have been corrected for the slow depolymerization that occurs after 55 s as described above. Symbols represent the data, i.e., the evolution with time of turbidity (+), GTP–microtubules (●), GDP-P_i–microtubules (▲), and GDP–microtubules (◇). Solid lines represent corresponding theoretical curves described by eqs 7 and 9, with the following values of the rate constants: $k_1 = 0.045$ s^{-1}, $k_2 = 0.06$ s^{-1}, and $k_3 = 0.02$ s^{-1}.

Since microtubules and flat sheets (on average 8 protofilaments wide) have an average length of 0.4 μm, i.e., contain 700 and 300 subunits respectively, and since the concentration of polymerized tubulin is 27 μM, the approximate concentration of elongating species is 27/500 = 0.05 μM, and a plausible value of k_+ is 0.2/0.05 = 4 μM^{-1} s^{-1} in MGM buffer, which is consistent with the previous determination (Carlier et al., 1987b).

Previous experiments indicated that GTP hydrolysis actually occurred vectorially, rather than randomly, on growing microtubules (Carlier et al., 1987b). As previously developed, a simple correspondence can be found between the value of the rate constant for GTP hydrolysis assuming that all n GTP subunits in the microtubule are active sites (random hydrolysis) and the value of the rate constant assuming there is only 1 active site/microtubule moving distally with time (vectorial model). In the latter case, this single site would have to hydrolyze at an n-fold higher rate than in the former case to account for the experimental data. Assuming an average of 700–300 GTP subunits/microtubule or sheet in our experiment (as checked below), the rate of hydrolysis in a vectorial model would be 20–50 s^{-1}, a value in good agreement with that found previously by an independent method (Carlier et al., 1987b). Although no evidence has been shown thus far for a vectorial mechanism in P_i release, the same reasoning could apply as well, leading to a plausible value of 6–15 s^{-1} for vectorial P_i release on a GDP-P_i subunit at the GDP-P_i/GDP boundary. Figures 7 and 10 show that at the early times (15 s) the measured amount of GDP-P_i subunits in microtubules is lower than the expected amount within the theoretical (random) model. This may correspond to a delay for the first subunits in the GDP-P_i stretch, to release P_i, followed by a faster vectorial reaction on distally adjacent subunits; in other words, this observation may support a vectorial P_i release.

Discussion

The experiments presented in this paper show that stretches of GTP- and GDP-P_i–tubulin units are transient components of microtubules in the early stages of tubulin polymerization. Analysis of the data indicates that P_i release is somewhat

slower than cleavage of GTP; therefore, microtubules growing at a fast rate have terminal GTP–subunits and subterminal GDP-P_i–subunits. The fact that, within a vectorial model in a regime of fast growth at high tubulin concentration, microtubules contain a large number of terminal GTP– and subterminal GDP-P_i–subunits does not support models of microtubule assembly within which GTP hydrolysis would be tightly coupled to the assembly process at any concentration of tubulin, i.e., would take place at an undefined very fast rate, except on the terminal subunit, which would never hydrolyze GTP (Walker et al., 1988; Bayley et al., 1990). The present data, however, show that when the rate of microtubule growth in MEM buffer does not exceed 2 μm/min at 37 °C, the GTP cap must be very small. In particular, they agree with previous observations of tight temporal coupling between microtubule elongation and GTP cleavage in a regime of slow growth only (Carlier et al., 1987b). More importantly, the evidence for the slow rate of P_i release suggests that, in a regime of slow growth where no appreciable GTP cap exists, terminal GDP-P_i subunits might be sufficient to stabilize microtubules. This GDP-P_i cap would account for the low critical concentration (same critical concentration at the two ends) derived from the tubulin concentration dependence of the rate of elongation measured during the periods of reversible slow growth of individual microtubules (Walker et al., 1988).

The success of the technique showing evidence for the GTP and GDP-P_i intermediates relies in part on the improvement of the glass filter assay. Two essential requirements were fulfilled. First, the short dead time of the filtration (approximately 2 s) is crucial. Former filtration techniques had a dead time, for processing the sample and filtering, of about 20 s (Carlier, 1988; Stewart et al., 1989), and reactions of rate constants in the range of 0.07 s^{-1} such as found here for GTP hydrolysis are 75% complete in 20 s, which explains the failure of the previous assay to detect more than a few percent of GTP or GDP-P_i subunits on microtubules. (Note anyhow that, with a dead time of 2 s, in the present experiment as much as 13% of a reaction with rate constant 0.07 s^{-1} is lost.) Second, a rapid rise in temperature, which ensures the explosive polymerization of many short microtubules, and hence the highest possible transient amount of polymerized GTP–subunits, also proved essential. Experiments (not shown) in which the test tube was not preheated led to a slower polymerization and smaller transient amounts of GTP– and GDP-P_i–microtubules, as also shown in the absence of taxol (Figure 9).

An important issue to be discussed is the relevance of the values found here for GTP hydrolysis and P_i release, under conditions of rapid nucleation and growth, to experiments documenting dynamic instability of individual microtubules that can be observed only under conditions of slow growth, i.e., when spontaneous nucleation is avoided. Evidently the rate constants measured refer to tubulin polymerized in short microtubules and sheets. The microtubular nature of the flat sheets (6–10 protofilaments wide) obtained in the first steps of microtubule assembly has been well established (Voter & Erickson, 1984) and is also apparent in Figure 4. Although of smaller size than conventional microtubules that contain 5000–10 000 subunits, these polymers are made up of 300–700 tubulin molecules, among which the proportion of edge subunits, i.e., those not entirely buried in the microtubular lattice, is larger than for long closed microtubules but does not exceed 20% of the polymerized subunits. Therefore, 80% of the tubulin polymerized in the presented experiments is involved in true microtubular tubulin–tubulin interactions; hence, we may trust that the rate constants found for GTP hydrolysis essentially pertain to the microtubule structure. This conclusion is further corroborated by the observation of a lower but measurable transient amount of GDP-P_i–tubulin on closed microtubules assembled under standard conditions, i.e., in the absence of taxol (Figure 9).

A related point concerns the validity of the turbidimetric method used to monitor the time course of assembly of such short polymers. Actually, Figure 4 documents that at 20 s, when the turbidity plateau is reached, the specific turbidity of the population of 0.4-μm-long microtubules is 77% of the specific turbidity of normal, several microns long microtubules, a result in agreement with Berne's calculations (Berne, 1974). The specific turbidity of the smaller sheets formed in the early steps of assembly is expected to be even lower. Turbidity therefore leads to an underestimated value of the real amount of polymerized subunits. Therefore, it is true that the polymerization rate constants derived fromthe turbidity data are probably somewhat lower than real values; consequently, the uncoupling measured between polymerization and GTP hydrolysis is also somewhat underestimated. Although turbidity in the present case does not give an accurate quantitative measurement of the kinetics of polymerization, it is worth noticing that the time course of polymerization followed by the filter assay correlates reasonably well with the turbidity recording.

The rates of GTP hydrolysis and P_i release are similar in two buffers in which microtubules exhibit very different dynamics. It is known that the presence of glycerol stabilizes microtubules by lowering the rate of dissociation of GDP–subunits. In the presence of glycerol, although GTP and GDP-P_i caps exist as shown in the present paper and consistent with previous works (Carlier et al., 1984, 1987b), microtubules are less dynamic because, due to the slower rate of GDP–tubulin dissociation from microtubule ends, the probability of rebuilding a cap of GDP-P_i subunits is high and extensive loss of several hundreds of subunits is a rare event above the critical concentration.

The rate constant found for GTP hydrolysis in the present work is 1 order of magnitude larger than the one derived earlier (Carlier & Pantaloni, 1981) from the analysis of the time courses of tubulin polymerization and GTP hydrolysis, in the absence of taxol and the presence of an excess of free GTP. Taxol is unlikely to cause a change in the rate of GTP hydrolysis (Carlier & Pantaloni, 1983) and be responsible for this discrepancy. Two other reasons may be invoked. First, in the presence of free GTP, a constant steady-state GTP hydrolysis is recorded following microtubule assembly. It was observed, as is also evident in the more recent data of O'Brien et al. (1987), that the steady-state GTP hydrolysis is established much later than the steady state of assembly. In our initial work (David-Pfeuty et al., 1978; Carlier & Pantaloni, 1981), it was assumed that GTP was hydrolyzed catalytically at microtubule ends; therefore, this constant rate was subtracted from the overall hydrolysis reaction to derive the burst phase of GTP hydrolysis accompanying assembly. However, this analysis now appears to be incorrect, since it was demonstrated later (Mitchison & Kirschner, 1984) that microtubules exhibit dynamic instability and therefore turn over more rapidly at steady state than predicted within classical models (even in glycerol-containing MGM buffer, 4-μm-long microtubules are renewed in 20–30 min); this fast turnover accounts for the high steady-state rate of GTP hydrolysis [it is easy to notice that the rate of GTP hydrolysis at steady state is a direct measurement of the extent of dynamic instability (Carlier et al., 1988)]. The previous analysis obviously led to an erro-

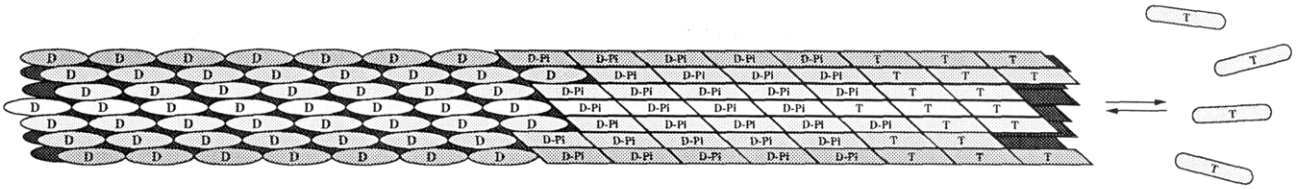

FIGURE 11: Schematic drawing of one end of a microtubule growing in the presence of GTP. The GTP–tubulin dimer and the polymerized GTP– (T), GDP-P_i– (D-P_i), and GDP– (D) tubulin subunits are represented with different shapes, which emphasize the more extensive intersubunit contacts in the GTP and GDP-P_i states than in the GDP state.

neously low value of the rate of GTP hydrolysis on microtubules, because dynamic instability does not develop until the late stages of assembly, upon approaching the critical concentration, and therefore does not interfere with the early stages of assembly. Another reason for the higher GTP hydrolysis pseudo-first-order rate constant found here is likely to be due to the vectorial mechanism of GTP hydrolysis on microtubules: within this mechanism, the apparent pseudo-first-order rate constant is proportional to the number of hydrolysis sites, i.e., related to microtubule number, which is 1 order of magnitude higher in the present work than in our former experiments. More recent works (Carlier et al., 1987; Caplow et al., 1985) favored a model within which GTP is hydrolyzed preferentially on a GTP subunit distally adjacent to a GDP-P_i subunit (Carlier et al., 1984; Caplow & Reid, 1985). This mechanism would result in a solid cap of GTP subunits separated from GDP-P_i subunits by a clean-cut boundary migrating toward the growing end at a rate of 40 s^{-1} (2 μm/min) at 30 °C under buffer conditions similar to the ones used here. If microtubules assembled with taxol have a quasiexponential length distribution centered around 0.4 μm average length (700 subunits), the measured pseudo-first-order hydrolysis rate constant of 0.065 s^{-1} would be consistent with 1 site/microtubule hydrolyzing GTP within a vectorial mechanism at a rate of $0.065 \times 700 = 45$ s^{-1}, which is consistent with the previous determination using a different technique (Carlier et al., 1987b).

If we assume that P_i release too is essentially a vectorial process, a microtubule in a regime of fast growth in MEM buffer (over 2 μm/min) would be made of a central core of GDP subunits followed distally by a first cap of GDP-P_i subunits and a second cap of terminal GTP subunits (Carlier, 1989), as illustrated in Figure 11. The GTP/GDP-P_i boundary would migrate distally at a rate of 40 subunits/s, while the GDP-P_i/GDP boundary would migrate at a slower rate (6–15 subunits/s, i.e., 0.3–0.7 μm/min), It has previously been shown that P_i had a low affinity ($K_D \sim 30$ mM) for microtubule GDP–subunits, while P_i analogues AlF_4^- and BeF_3^- bind tightly (Carlier et al., 1988; Caplow et al., 1988a, 1989). In a regime of slow growth, i.e., in a range of tubulin concentration where the splitting of GTP appears to be tightly coupled to the elongation process (Carlier et al., 1987b), a single cap of slowly dissociating GDP-P_i subunits exists at microtubule ends. Keeping with the present data and the hypothesis of a simple vectorial P_i release, the size of the GDP-P_i cap should increase steadily with time when the rate of growth is above 0.3–0.7 μm/min. Consequently, dilution-induced disassembly of microtubules is expected to show a delay preceding rapid depolymerization of the GDP core. The delay corresponds to the time necessary for the vectorial wave of P_i release to reach the end of the microtubule and for GDP-P_i subunits to dissociate; therefore, it should increase linearly with the duration of the period of growth preceding dilution. Such a delay of 6–15 s has actually been observed (Walker et al., 1989), in agreement with the existence of a measurable cap, but its length does not vary very steeply with the pregrowth period, suggesting that the size of the stabilizing cap is limited. A reasonable explanation is that a strictly vectorial model for P_i release does not apply and a low probability also exists for random P_i release, which actually is a necessary event at least to initiate a GDP/GDP-P_i boundary. This reaction may generate more than one GDP-P_i/GDP interface per microtubule. As an example, a similar mixed vectorial + random hydrolysis mechanism has been found for Mg-ATP–actin (Carlier et al., 1987c). As a result, the first GDP-P_i/GDP interface starting from the distal end of a microtubule could not be at a position deeper than a certain number of subunits, depending on the probability of random P_i release in a stretch of GDP-P_i subunits. For example if the rate of vectorial P_i release is 10 s^{-1}, a maximum delay of 10 s in dilution-induced depolymerization would indicate that the size of the GDP-P_i cap is limited to 100 subunits.

The low value of the rate constant for P_i dissociation from GDP-P_i subunits found in this work implies an unusual very slow rate constant for P_i association to GDP–subunits. It is therefore likely that, like on myosin (Stein et al., 1985) and actin (Carlier & Pantaloni, 1986), P_i release on microtubules is rate-limited by a conformational change of a central GDP-P* transition complex into the GDP-P_i entity from which P_i would dissociate at a fast rate. Under physiological conditions (2 mM inorganic phosphate, pH 7), phosphate is not appreciably bound to microtubules; the stabilization of the microtubule lattice by P_i is therefore exerted, in cells, exclusively kinetically, via the GDP-P_i transient state. Previous experiments using phosphate analogues have shown that GDP-P_i subunits dissociated from microtubule ends at a very slow rate; hence, even a small GDP-P_i cap is effective to prevent the catastrophic depolymerization of the GDP core. On the other hand, the rate of dissociation of GTP–subunits is unknown; GTP–subunits could be energetically and structurally identical with GDP-P_i–subunits and depolymerize at the same slow rate or could depolymerize faster, as suggested by the upward curvature of the $J(c)$ function in a regime of fast growth (Carlier et al., 1987b). More work is needed to test these possibilities, since the relative values of the rate constants for dissociation of GTP– and GDP-P_i–subunits from microtubule ends are important parameters in the modelization of microtubule dynamics.

Finally it is worth noticing the qualitative similarity and quantitative difference between the actin and the microtubule systems. Transient F-ATP–actin and F-ADP-P_i–actin filaments are intermediates in the polymerization of ATP–actin, and P_i release is also linked to the destabilization of the filament structure (Carlier & Pantaloni, 1988; Korn et al., 1987). However, P_i release is 2 orders of magnitude faster on microtubules than on actin, which may interestingly be correlated with the more accentuated dynamics and oscillatory behavior of microtubules.

REFERENCES

Bayley, P. M., Schilstra, M. J., & Martin, S. R. (1990) *J. Cell Sci. 95*, 33–48.

Berne, B. J. (1974) *J. Mol. Biol. 89*, 755–758.
Caplow, M., & Reid, Z. (1985) *Proc. Natl. Acad. Sci. U.S.A. 82*, 3267–3271.
Caplow, M., Shanks, J., & Brylawski, B. P. (1985) *Can. J. Biochem. 63*, 422–429.
Caplow, M., Shanks, J., & Ruhlen, R. L. (1988a) *J. Biol. Chem. 263*, 10344–10352.
Caplow, M., Shanks, J., Breidenbach, S., & Ruhlen, R. L. (1988b) *J. Biol. Chem. 263*, 10943–10951.
Caplow, M., Ruhlen, R., Shanks, J., Walker, R. A., & Salmon, E. D. (1989) *Biochemistry 28*, 8136–8141.
Carlier, M.-F. (1988) *Cell Biophys. 12*, 105–117.
Carlier, M.-F. (1989) *Int. Rev. Cytol. 115*, 139–170.
Carlier, M.-F., & Pantaloni, D. (1978) *Biochemistry 17*, 1908–1915.
Carlier, M.-F., & Pantaloni, D. (1981) *Biochemistry 20*, 1924–1932.
Carlier, M.-F., & Pantaloni, D. (1983) *Biochemistry 22*, 4814–4822.
Carlier, M.-F., & Pantaloni, D. (1986) *Biochemistry 25*, 7789–7792.
Carlier, M.-F., & Pantaloni, D. (1988) *J. Biol. Chem. 263*, 817–825.
Carlier, M.-F., Hill, T. L. & Chen, Y. (1984) *Proc. Natl. Acad. Sci. U.S.A. 81*, 772–776.
Carlier, M.-F., Melki, R., Pantaloni, D., Hill, T. L., & Chen, Y. (1987a) *Proc. Natl. Acad. Sci. U.S.A. 84*, 5257–5261.
Carlier, M.-F., Didry, D., & Pantaloni, D. (1987b) *Biochemistry 26*, 4428–4437.
Carlier, M.-F., Pantaloni, D., & Korn, E. D. (1987c) *J. Biol. Chem. 262*, 3052–3059.
Carlier, M.-F., Didry, D., Melki, R., Chabre, M., & Pantaloni, D. (1988) *Biochemistry 27*, 3555–3559.
Carlier, M.-F., Didry, D., Simmon, C., & Pantaloni, D. (1989) *Biochemistry 28*, 1783–1791.
David-Pfeuty, T., Erickson, H. P., & Pantaloni, D. (1977) *Proc. Natl. Acad. Sci. U.S.A. 74*, 5372–5376.
Detrich, H. W., III, & Williams, R. C. (1978) *Biochemistry 17*, 3900–3907.
Detrich, H. W., III, Jordan, M. A., Wilson, L., & Williams, R. C. (1985) *J. Biol. Chem. 260*, 9479–9490.
Gaskin, F., Cantor, C. R., & Shelanski, M. L. (1974) *J. Mol. Biol. 119*, 737–758.
Hamel, E., Lustbader, J., & Lin, C. M. (1984) *Biochemistry 23*, 5314–5325.
Hill, T. L. (1985) *Proc. Natl. Acad. Sci. U.S.A. 82*, 431–435.
Hill, T. L. (1986) *Biophys. J. 49*, 981–986.
Hill, T. L. (1987) *Linear Aggregation Theory in Biology* (Rich, A., Ed.) Springer-Verlag, New York.
Horio, T., & Hotani, H. (1986) *Nature 321*, 605–607.
Huitorel, P., & Pantaloni, D. (1985) *Eur. J. Biochem. 150*, 265–269.
Karecla, P., Hirst, E., & Bayley, P. (1989) *J. Cell Sci. 94*, 479–488.
Korn, E. D., Carlier, M.-F., & Pantaloni, D. (1987) *Science 238*, 638–644.
Krauhs, E., Little, M., Kempf, T., Hofer Warbinek, R., Ade, W., & Ponstingl, H. (1981) *Proc. Natl. Acad. Sci. U.S.A. 78*, 4156–4160.
Mitchison, T., & Kirschner, M. W. (1984) *Nature 312*, 237–242.
O'Brien, E. T., Voter, W. A., & Erickson, H. P. (1987) *Biochemistry 26*, 4148–4156.
Pantaloni, D., Hill, T. L., Carlier, M.-F., & Korn, E. D. (1985) *Proc. Natl. Acad. Sci. U.S.A.* 7207–7211.
Schilstra, M. J., Martin, S. R., & Bayley, P. M. (1987) *Biochem. Biophys. Res. Commun. 147*, 588–595.
Shelanski, M. L., Gaskin, F., & Cantor, C. R. (1973) *Proc. Natl. Acad. Sci. U.S.A. 70*, 765–768.
Sherline, P., Bodwin, C. K., & Kipnis, D. M. (1974) *Anal. Biochem. 62*, 400–407.
Stein, L. A., Greene, L. E., Chock, P. B., & Eisenberg, E. (1985) *Biochemistry 24*, 1357–1363.
Stewart, R. J., Farrell, K. W., & Wilson, L. (1989) *J. Cell Biol. 107*, 241a.
Thompson, W. C., Wilson, L., & Purich, D. L. (1981) *Cell Muscle Motil. 1*, 445–454.
Voter, W. A., & Erickson, H. P. (1984) *J. Biol. Chem. 259*, 10430–10438.
Walker, R. A., O'Brien, E. T., Pryer, N. K., Soboeiro, M., Voter, W. A., Erickson, H. P., & Salmon, E. D. (1988) *J. Cell Biol. 107*, 1437–1448.
Walker, R. A., Pryer, N. K. & Salmon, E. D. (1989) *J. Cell Biol. 109*, 342a.
Wani, M. C., Taylor, H. L., Wall, M. E., Coggon, P., & MacPhail, A. T. (1971) *J. Am. Chem. Soc. 93*, 2325–2327.
Weingarten, M. D., Lockwood, A. H., Hwo, S. Y., & Kirschner, M. W. (1975) *Proc. Natl. Acad. Sci. U.S.A. 72*, 1858–1862.
Williams, R. C., Jr., & Rone, L. S. (1989) *J. Biol. Chem. 264*, 1663–1670.
Wilson, L., Snyder, B. K., Thompson, W. C., & Margolis, R. L. (1982) *Methods Cell Biol. 24*, 159–169.
Wilson, L., Miller, H. P., Farrell, K. W., Snyder, K. B., Thompson, W. C., & Purich, D. L. (1985) *Biochemistry 24*, 5254–5262.